photonics

MDPI

Article

Terahertz Generation by Optical Rectification of 780 nm Laser Pulses in Pure and Sc-Doped $ZnGeP_2$ Crystals

Vladimir Voevodin [1,2], Svetlana Bereznaya [3], Yury S. Sarkisov [4], Nikolay N. Yudin [2,3,5] and Sergey Yu. Sarkisov [1,3,*]

1 Synchrotron Radiation Detector Laboratory, R&D Center "Advanced Electronic Technologies", Tomsk State University, Tomsk 634050, Russia
2 LLC Laboratory of Optical Crystals, Tomsk 634040, Russia
3 Laboratory for Terahertz Research, Tomsk State University, Tomsk 634050, Russia
4 Department of Physics, Chemistry and Theoretical Mechanics, Tomsk State University of Architecture and Building, Tomsk 634003, Russia
5 Laboratory for Radiophysical and Optical Methods of Environmental Studies, Tomsk State University, Tomsk 634050, Russia
* Correspondence: sarkisov@mail.tsu.ru

Abstract: Terahertz wave generation through the optical rectification of 780 nm femtosecond laser pulses in $ZnGeP_2$ crystals has been studied. All of the possible interactions of types I and II were analyzed by modeling and experimentally. We demonstrate the possibility of broadband "low-frequency" terahertz generation by an *ee–e* interaction (with two pumping waves and a generated terahertz wave; all of these had extraordinary polarization in the crystal) and "high-frequency" terahertz generation by an *oe–e* interaction. The arising possibility of achieving the narrowing of the terahertz generation bandwidth at the *oe–e* interaction using thicker $ZnGeP_2$ crystals is experimentally confirmed. It has been found that the thermal annealing of as-grown $ZnGeP_2$ crystals and their doping with a 0.01 mass % of Sc reduces the absorption in the "anomalous absorption" region (λ = 0.62–3 μm). The terahertz generation by the *oo–e* interaction in (110) $ZnGeP_2$:Sc and the as-grown $ZnGeP_2$ crystals of equal thicknesses was compared. It has been found that $ZnGeP_2$:Sc is more efficient for 780 nm femtosecond laser pulses optical rectification.

Keywords: $ZnGeP_2$; terahertz time-domain spectroscopy; nonlinear crystal; doping; terahertz generation; optical rectification; phase matching

check for updates

Citation: Voevodin, V.; Bereznaya, S.; Sarkisov, Y.S.; Yudin, N.N.; Sarkisov, S.Y. Terahertz Generation by Optical Rectification of 780 nm Laser Pulses in Pure and Sc-Doped $ZnGeP_2$ Crystals. *Photonics* **2022**, *9*, 863. https://doi.org/10.3390/photonics9110863

Received: 30 October 2022
Accepted: 12 November 2022
Published: 16 November 2022

Publisher's Note: MDPI stays neutral with regard to jurisdictional claims in published maps and institutional affiliations.

Copyright: © 2022 by the authors. Licensee MDPI, Basel, Switzerland. This article is an open access article distributed under the terms and conditions of the Creative Commons Attribution (CC BY) license (https://creativecommons.org/licenses/by/4.0/).

1. Introduction

$ZnGeP_2$ crystals with the chalcopyrite structure have been grown and used in nonlinear optics for 50 years [1–3]. It is known that this crystal has a high nonlinear susceptibility $d_{14} \approx d_{36}$ = 75 pm/V, a thermal conductivity of 0.35 W/(cm·K), a maximum transparency range of 3–8 μm (with $\alpha < 0.05$ cm^{-1} for the best samples), positive birefringence in the IR range n_e-$n_o \approx 0.04$, and high damage thresholds (up to 2–3 J/cm^2 for 30 ns pulses at λ = 2.05 μm for the best samples) [4,5]. To date, the development of the methods of synthesis [4–6] and the crystallization by the vertical Bridgman method [4,6] and the horizontal method of directed cooling [5] has led to the possibility of obtaining $ZnGeP_2$ ingots up to 50 mm in diameter and up to 140–200 mm in length.

Nevertheless, the development of growth technology for obtaining more perfect crystals with an enhanced damage threshold and a lower level of absorption in the wavelength range of 0.62–3 μm and in the terahertz range remains relevant. The crystals that are grown using modern technology have an anomalous absorption in the region of 0.62–3 μm with an absorption maximum about wavelength λ = 1 μm. This absorption is associated with the presence of point defects in the as-grown material [7]. Singly ionized zinc vacancies can act as such defects [4,5,7]. The use of thermal annealing or irradiation with high-energy

electrons reduces the absorption in the $ZnGeP_2$ crystals [4]. Irradiation with high-energy electrons leads to the formation of radiation defects and the pinning of the Fermi level near the local electroneutrality level, which leads to the recharging of the acceptor levels and a decrease in their optical activity [7]. It is assumed [4] that irradiation leads to the motion of interstitial atoms and the formation of Frenkel complexes with acceptor defects. It is also supposed that $ZnGeP_2$ ingots of a large size contain fewer zinc vacancies because fewer volatile components, in particular zinc, are deposited on the walls of the ampoules during synthesis and crystallization [4,5]. To prevent the decomposition of the material, synthesis, as well as thermal annealing, is often carried out with the addition of ZnP_2, P, or $ZnGeP_2$ powders to the ampoule [8,9]. It is noted that optical damage occurs more often on the surface [4,5,10]. The value of the damage threshold strongly depends on the quality of the grown crystals and the polishing technology.

Currently, $ZnGeP_2$ crystals are mainly used to generate the harmonics of CO and CO_2 lasers and in optical parametric oscillators (OPO) with pumping at wavelengths of 2.05–2.94 μm and for the generation of radiation in the region of 3–10 μm. Such applications require crystals with a high damage threshold, large working aperture and low absorption in the 2–10 μm wavelength range. Another possible application of $ZnGeP_2$ crystals is the generation of terahertz radiation [11]. This requires crystals with a low absorption capacity in the given spectral range, and in the case of their generation by the optical rectification of femtosecond laser pulses, with a low dispersion of absorption coefficients [12,13]. To calculate the phase-matching conditions, it is important to know the wavelength dependences of the refractive indices for the ordinary and extraordinary waves. In this case, in contrast to the IR range, in which there are sufficiently reliable data for the spectral dependences of the refractive indices of $ZnGeP_2$ crystals [14], there are some contradictions in the published data in the terahertz frequency range [15,16]. In particular, it was found [8,15,16] that in the terahertz frequency range, the positive birefringence of $ZnGeP_2$ in the IR range is replaced by a negative one. Due to their optical properties, the $ZnGeP_2$ crystals are less advantageous for their application in the optical rectification of Ti:Sapphire laser radiation with λ = 750–850 nm. The majority of these studies have been devoted to the optical rectification of laser pulses with wavelengths of 1.1–2.4 μm. Additionally, a low birefringence capacity and a rather high difference between the optical group and terahertz refractive indices hampers the realization of phase-matching and high conversion efficiency expected for the material with high values for the components of the second-order nonlinear susceptibility tensor. To solve this problem in [17], a noncollinear scheme for optical rectification was proposed to maximize the θ (the angle between the laser wavevector and *c*-axis inside the crystal), and therefore, the effective nonlinearity for the *oe–o* and *oe–e* interactions. The optical rectification of laser pulses at wavelengths that were from 800 to 1550 nm was studied [18], and it was found that $ZnGeP_2$, having a rather high adsorption rate (17.88 cm^{-1} @ 800 nm, 17.01 cm^{-1} @ 1300 nm and 15.87 cm^{-1} @ 1550 nm) is less efficient than the $CdSiP_2$ and $CdGeP_2$ crystals. One of the very few works where an 800 nm femtosecond pulse optical rectification in $ZnGeP_2$ was studied is [19], where also the electro-optical sampling of the terahertz transients in $ZnGeP_2$ was studied.

In the majority of cases for the 800 nm laser pulses, the optical rectification $ZnGeP_2$ crystals definitely lose to analogues such as GaSe, with the latter having a high transparency at both the terahertz and optical pump wavelengths, a high birefringence capacity and a large damage threshold for terahertz radiation [13,14]. Thus, the GaSe crystals are widely used in various terahertz and IR experiments, such as pump-probe schemes, terahertz and IR nanoscopy and spectroscopy [20]. The possible advantage of using $ZnGeP_2$ crystals could be the possibility to cut at phase-matching angles, their higher mechanical hardness and the availability of antireflection coatings. On the other hand, some experimental realizations of optical antireflection coatings on GaSe have been performed during the last few years [21,22]. High terahertz refractive indices for both GaSe and $ZnGeP_2$ and difficulties in producing the antireflection coatings for terahertz radiation using standard

methods because of the required large thickness of the deposited films leads to high losses in the generated terahertz pulses.

The doping of nonlinear crystals is one of the ways to modify their transparency, mechanical properties, dispersion and nonlinearity [13,14]. The doping of $ZnGeP_2$ crystals for optical applications has not been studied intensively.

In the present work, we study the effect of thermal annealing and Sc doping on the optical transmission and refractive indices of $ZnGeP_2$ crystals in the optical and terahertz frequency range. Then terahertz generation through the optical rectification of 780 nm femtosecond laser pulses in these crystals is studied. All of the possible interactions of types I and II of nonlinear optical rectification have been studied both by modeling and by experiments. We find the advantageous interactions and phase-matching angles for (100) and (110) $ZnGeP_2$ crystals, taking into account the angular dependence of reflection, effective nonlinearity and the required terahertz frequency range.

2. Experimental Methods

2.1. Sample Preparation

To grow the $ZnGeP_2$ crystals, high-purity initial components (Zn, Ge and P of 6N grade) were taken. The crystals were grown using the vertical Bridgman method [6,8]. Two growth cycles were performed. The thermal annealing of the samples grown in the experiment N1 was carried out in sealed ampoules with the addition of $ZnGeP_2$ powder to create a vapor phase pressure in the ampule which prevented the decomposition of the material. The annealings were carried out at temperatures of 575–700 °C for 300–400 h. In experiment N2, for the synthesis Zn, Ge and P of 5N grade were used. The synthesized material was divided in to two parts. To one part (50% of mass of synthesized material) scandium was added in an amount of 0.01 mass % of the total charge. Then, two ingots were crystallized using the same setup and experimental growth conditions.

The slabs of annealed $ZnGeP_2$ with thicknesses of 200, 500 and 800 μm were prepared by cutting them along the (001) plane and polishing them. The slabs with thicknesses of 400 μm cut along the (110) plane were prepared from pure and scandium-doped $ZnGeP_2$. The samples did not have antireflection coatings.

2.2. Optical Absorption Measurement

The optical transmission spectra were measured using a UV-3600i-Plus (Shimadzu, Kyoto, Japan) spectrometer in 0.6–2.5 μm range. From the measured transmission spectra $T(\lambda)$, the absorption coefficients $\alpha(\lambda)$ were calculated by solving, numerically, a system of two equations (which are below), taking into account the multiple reflections in the thin samples and reflection $R(\lambda)$ from an absorbing medium:

$$\alpha(\lambda) = -\frac{1}{d}\ln\left(\frac{\sqrt{(1-R(\lambda))^4 + 4T^2(\lambda)R^2(\lambda)} - (1-R(\lambda))^2}{2T(\lambda)R^2(\lambda)}\right) \quad (1)$$

and

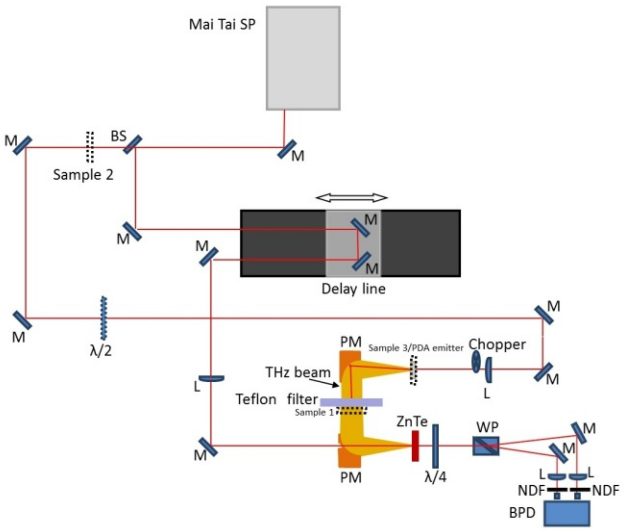
$$R(\lambda) = \frac{(n(\lambda)-1)^2 + \left(\frac{\lambda\alpha(\lambda)}{4\pi}\right)^2}{(n(\lambda)+1)^2 + \left(\frac{\lambda\alpha(\lambda)}{4\pi}\right)^2} \quad (2)$$

where the refractive indices were calculated as $n(\lambda) = n_o(\lambda) + 0.03$, and $n_o(\lambda)$ was taken from [23]. In Equations (1) and (2), $R(\lambda)$ is intensity reflection coefficient for the $ZnGeP_2$/air interface, and $T(\lambda)$ is the transmission coefficient which is influenced by multiple reflections. The measurements were carried out on (100) oriented samples in unpolarized light at a normal incidence.

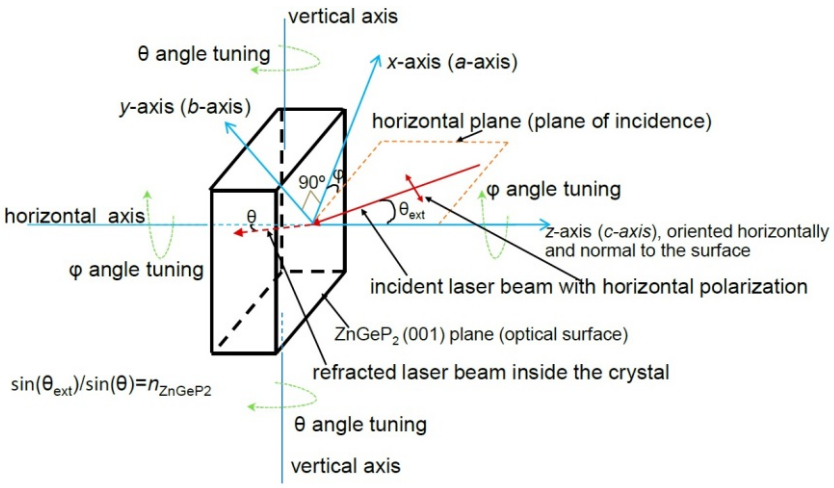
2.3. THz-TDS Measurements

The experiments were conducted using the conventional terahertz time-domain spectroscopy (THz-TDS) setup [24] that is in Figure 1a. To obtain the terahertz pulses for the

terahertz transmission measurements and tests of the nonlinear crystals, the laser pulses of Mai Tai SP (Spectra-Physics, Milpitas, CA, USA; λ = 780 nm, τ~100 fs) with a horizontal polarization (parallel to the optical table's surface) were used. For the detection step, an electro-optical (110)-cut ZnTe crystal with a zinc blende structureand d = 1100 μm was used. The Teflon filter (Figure 1a) was used to block the residual 780 nm laser radiation and transmit the emitted terahertz pulse. The delay line (Figure 1a) was a motorized linear stage Model IMS600CCHA (Newport, Milpitas, CA, USA) with an XPS C4 controller (Newport, Milpitas, CA, USA), and this was used to scan the terahertz waveforms by changing the optical path of the laser probe pulse with a step of 5 or 10 μm. The difference in the intensity of the horizontally and vertically polarized components of the probing laser pulse separated by the Wollaston prism (Figure 1a) was measured using the Model 2007 Nirvana balanced detector (New Focus, Milpitas, CA, USA).

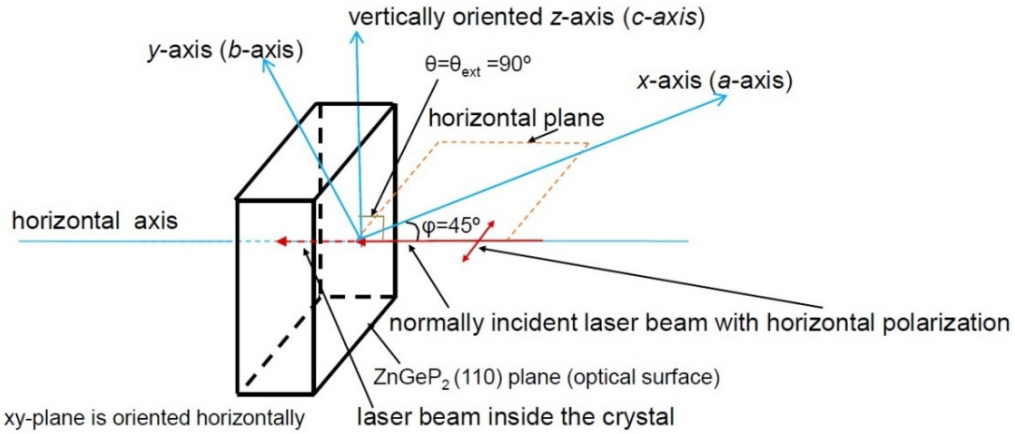


(**a**)



(**b**)

Figure 1. *Cont*.



(**c**)

Figure 1. (**a**) Scheme of the experimental setup: L—lens; M—mirror; BS—beam splitter; PM—parabolic mirror; λ/2—halfwave plate; λ/4—quaterwave plate; WP—Wollaston prism; NDF—neutral density filter; PDA emitter—SI-GaAs photoconductive dipole antenna terahertz emitter; BPD—balanced photodetector. The components that were introduced only for particular experiments are shown with dashed boarders. Orientation of crystallographic (*a*, *b* and *c*) as well as crystal physical (*x*, *y* and *z*) axes with respect to incident laser beam and its polarization during optical rectification experiments for (001) (**b**) and (110) (**c**) oriented $ZnGeP_2$ samples.

To measure the terahertz dielectric properties, the $ZnGeP_2$ crystals were placed just after the teflon filter ("Sample 1" in Figure 1a), normally, to the terahertz beam (SI-GaAs photoconductive dipole antenna was used as a terahertz emitter in this case), and the terahertz spectra were recorded.

The measurements of the group refractive indices at a 780 nm wavelength in the $ZnGeP_2$ crystals were made in the following way. The (100)- or the (110)-oriented sample was introduced to the laser beam which was travelling to the PDA ("Sample 2" in Figure 1a). Then, the terahertz waveform was recorded. By comparing the waveforms that were recorded with and without the sample, the time shift Δt related to the pump beam delay in the sample was measured. This delay was determined by the sample group refractive index and its thickness. The ordinary group refractive index was measured with the sample orientation when the optical axis *c* was oriented vertically (perpendicular to laser beam polarization), and the extraordinary group refractive index was measured for the sample when the optical axis *c* was oriented horizontally (parallel to laser beam polarization). Then, the group refractive index was calculated as:

$$n_{gr} = \Delta t \cdot c/d + 1 \quad (3)$$

where *c* is speed of light and *d* is sample thickness.

When we were performing the optical rectification experiments, the (001)-cut $ZnGeP_2$ crystals ("Sample 3" in Figure 1a) with the optical axis *c* that was perpendicular to the optical surface were tilted around a vertical direction to set the required external phase-matching (θ_{ext}) angles, and these were optimized by the azimuth angle φ (the angle between the projection of extraordinary polarization component of a beam to *xy*-plane and the *x*-axis) for a maximum signal to be obtained (see Figure 1b). To realize the *eo* (type II) phase matching, a λ/2 plate (Figure 1a) was placed onto the laser beam before the nonlinear crystal with its optical axis tilted by 22.5 degrees with respect to the horizontal direction to rotate the laser polarization direction by 45 degrees. The output terahertz polarization was controlled by a wire-grid polarizer.

The (110) $ZnGeP_2$ crystals ("Sample 3" in Figure 1) with an optical axis *c* which was lying within the optical surface and *x* axis that was oriented at 45° to the optical surface

were placed normally to the incident laser beam with the optical axis *c* being oriented vertically and the *x* axis being oriented in horizontal plane, thus, setting the external phase-matching (θ = 90°) and azimuth angle φ = 45° and promoting the *oo–e* interaction (see Figure 1c).

3. Results and Discussion

In our experiments, the ordinary group refractive index that was measured was 3.95, and extraordinary group refractive index was 4.06 at λ = 780 nm for the annealed $ZnGeP_2$ crystals, while their values which were calculated using $n_o(\lambda)$ and $n_e(\lambda)$ from [23] were 3.919 and 4.034, respectively. Taking into account that for the majority of the samples the measured terahertz refractive indices (Figure 2a) were also about 0.03 higher than it follows from $n_o(\lambda)$ and $n_e(\lambda)$ in [23], in the further calculations we used dispersion relations from [23] but they were shifted 0.03 upwards in both of the optical and terahertz ranges, i.e., $n_o(\lambda) = n_o(\lambda) + 0.03$ and $n_e(\lambda) = n_e(\lambda) + 0.03$. From our measurements (in particular, the data in Figure 2a), it follows that refractive indices in $ZnGeP_2$ can be slightly different depending on the growth technology and the chemical impurity content. Additionally, the absorption (Figure 2b) differs; it is 1 cm^{-1} at ν = 1 THz for the Sc-doped samples and 3 cm^{-1} for the as-grown and annealed samples.

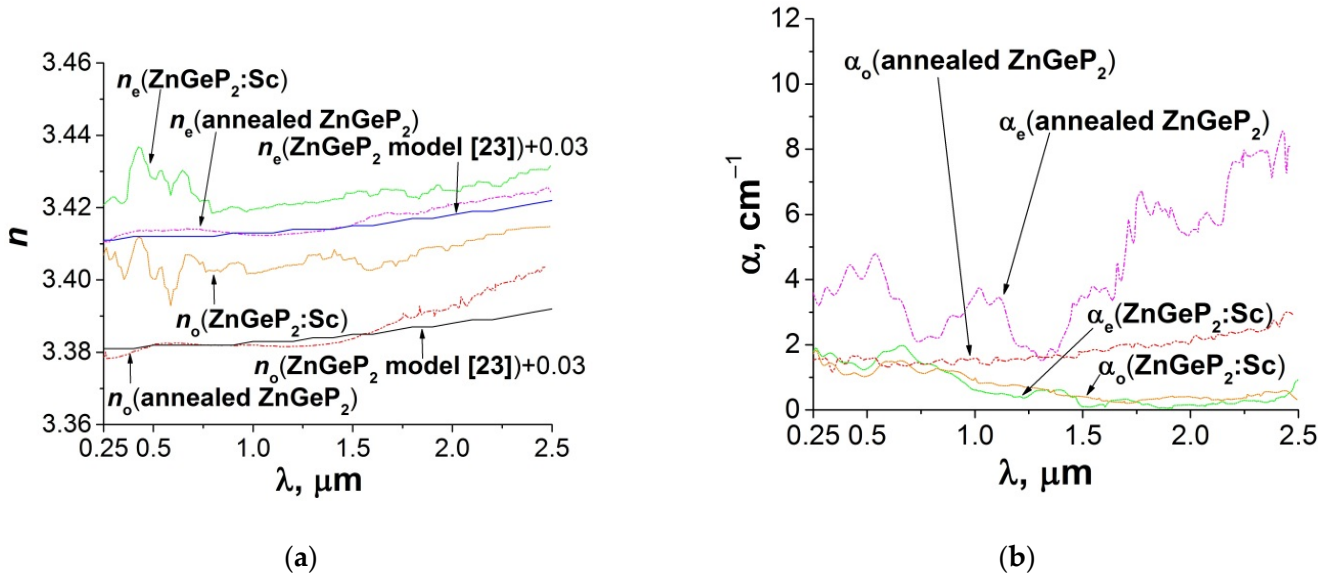


Figure 2. (**a**) The terahertz refractive indices and (**b**) absorption coefficients measured in annealed $ZnGeP_2$ (N1) and $ZnGeP_2$:Sc (N2) crystals. In panel (**a**), also model ordinary and extraordinary refractive indices ($n_o(\lambda)$ and $n_e(\lambda)$ taken from [23] and shifted by 0.03 upwards) are plotted.

It was found that the thermal annealing of the as-grown $ZnGeP_2$ crystals and their doping with only a 0.01 mass % Sc reduces the absorption in the "anomalous absorption" region (Figure 3). Both annealing and Sc doping can lead to the formation and redistribution of point defects, leading to the Fermi level being pinned, as proposed in [7]. It is also seen that at λ = 780 nm, the level of absorption is still high, and it equals 7.5 cm^{-1} for the annealed crystals, 11.5 cm^{-1} for the Sc-doped crystals and 21 cm^{-1} for the as-grown (N2) $ZnGeP_2$.

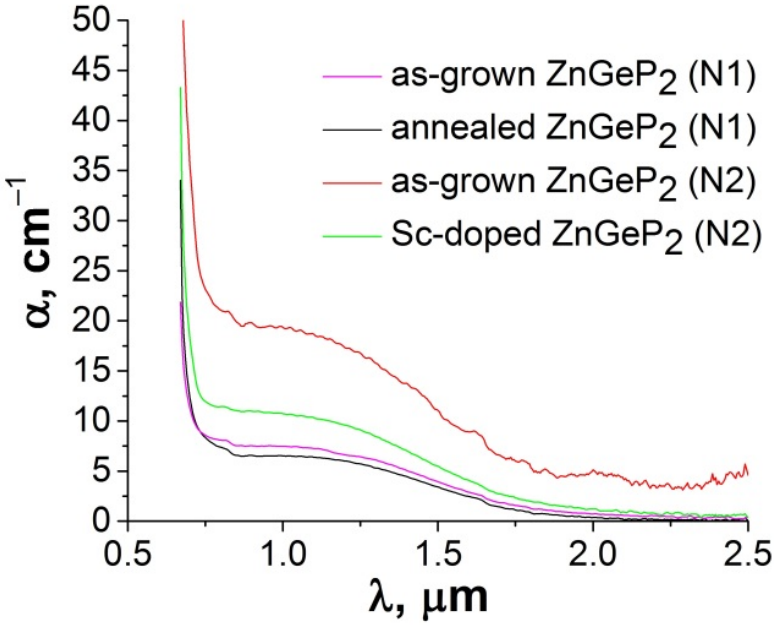


Figure 3. The optical absorption measured in as-grown and annealed $ZnGeP_2$ (N1) and in the reference and Sc-doped $ZnGeP_2$ (N2) crystals.

To investigate the influence of the crystal thickness, the polarization of the interacting waves and the phase-matching angles, a series of experimental measurements and model calculations were carried out. Firstly, we calculated the phase-matching conditions by taking into account the following. The phase-matching condition for a crystal of thickness d can be expressed as:

$$N\pi \leq |\Delta k| \cdot d \leq (N+1)\pi \tag{4}$$

where N = 0,2,4. When we were analyzing the phase-matching conditions, we considered the case of N = 0 for simplicity. For the *ee–o*, *ee–e*, *oo–o* and *oo–e* interactions of type I (when both incident laser beams have the same polarization), the phase mismatch can be written as [12,13,25]:

$$\Delta k(\nu, \lambda, \theta) = [n_{gr}(\lambda, \theta) - n_{THz}(\nu, \theta)] \cdot 2\pi\nu/c. \tag{5}$$

Here, ν is terahertz frequency, n_{gr} is the group refractive index and λ is the laser central wavelength. The group refractive index is calculated as:

$$n_{gr}(\lambda) = n(\lambda) - \lambda \frac{dn(\lambda)}{d\lambda}|_{\lambda} \tag{6}$$

In the case of the different polarizations of the laser pulse components participating in the nonlinear process (*eo–o*, *eo–e*, *oe–o*, *oe–e* interactions of type II), the phase mismatch (5) can be written the same way, but the group refractive index must be substituted by the effective function [12,13]:

$$n_{vis} = (n(\nu_{opt}) \cdot \nu_{opt} - n(\nu_{opt} - \nu) \cdot (\nu_{opt} - \nu))/\nu \tag{7}$$

According to the expressions (5–7), the calculated phase-matching conditions for all of the possible interactions are provided in Figure 4.

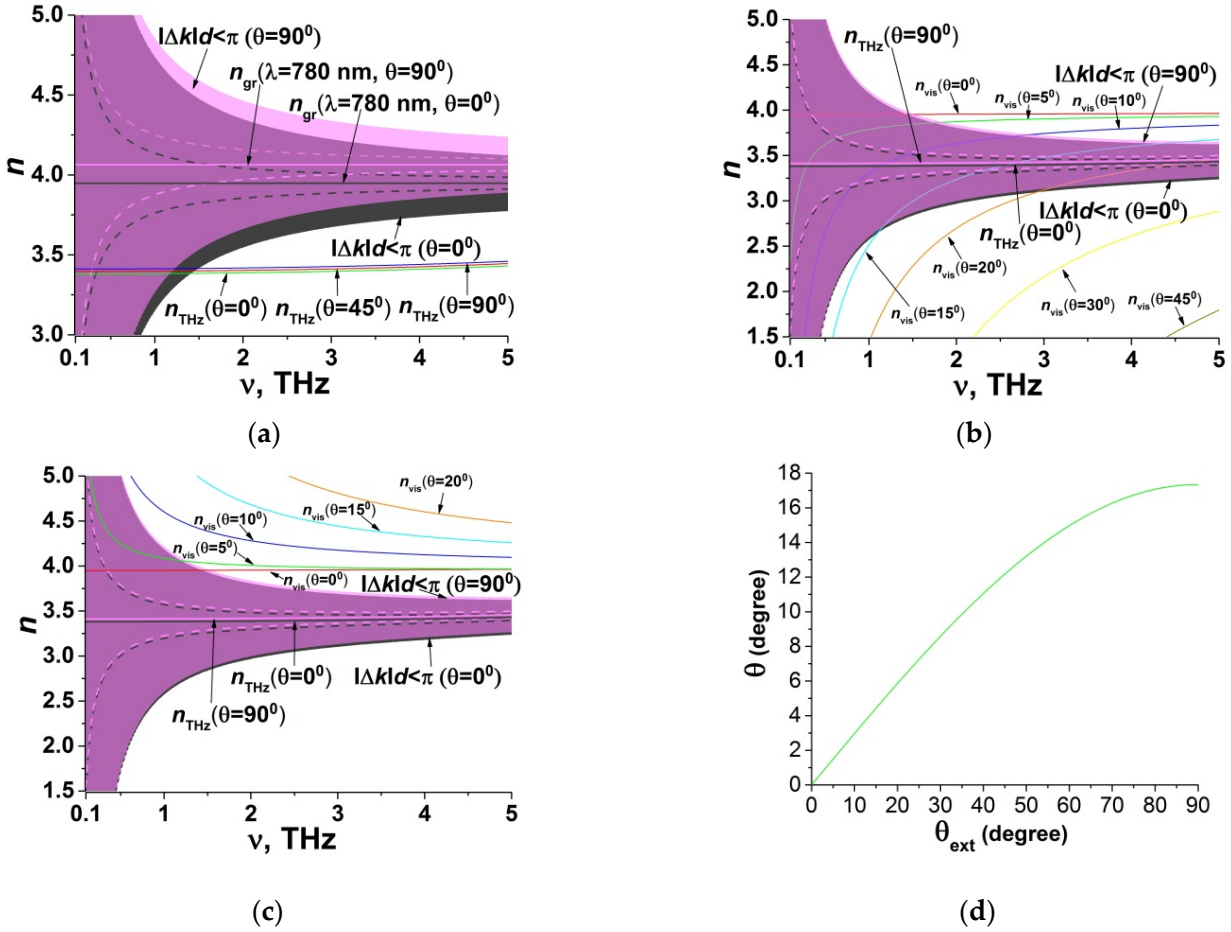


Figure 4. The terahertz and optical group refractive indices (**a**) and terahertz refractive indices and calculated $n_{vis}(\theta)$ (**b**) and (**c**) in $ZnGeP_2$ crystals for various θ angles. Dark grey and semi-transparent magenta color-filled areas indicate where condition (4) is fulfilled for the crystals with thicknesses of 200 μm at θ = 0° and θ = 90°, respectively; dark grey and magenta dashed lines indicate the corresponding boundaries for the crystal thickness of 800 μm. Here, panel (**a**) illustrates the phase matching conditions for all of the interactions of type I, panel (**b**) illustrates *oe–o* and *oe–e* interactions of type II, panel (**c**) illustrates *eo–o* and *eo–e* interactions of type II. Panel (**d**) illustrates the relationship between external angle of incidence θ_{ext} and phase-matching angle θ for (001) $ZnGeP_2$ crystal.

In the plots (Figure 4a–c), the semi-transparent magenta (dark grey)-filled area indicates where curves n_{THz} (θ) or n_{vis}(θ) at θ = 90° (θ = 0 °) should lie to fulfill the condition (4) (N = 0) for a crystal of a thickness d = 200 μm. For the intermediate angles of 0° < θ < 90°, the position of the filled areas would be in between those of the shown ones for these two critical angles (it is seen that their positions do not change significantly). Obviously for the thicker crystals, the phase-matching areas would be narrower than that which is illustrated by the boundaries for a crystal of a thickness d = 800 μm (the dashed lines of the same magenta and dark grey colors). Clearly, for the ordinary participating waves, the color-filled areas, n_{THz}(θ) or n_{vis}(θ) for θ = 0° at any θ values should be considered since for the ordinary waves there is no refractive index angular dependence.

As it can be seen, the angular dependence of the phase matching for all of the type I interactions is weak for the $ZnGeP_2$ crystals because of their low birefringence capacity and the large differences in the n_{gr}(λ = 780 nm)-n_{THz}(θ) (about 0.6, (Figure 4a). The condition (4) is fulfilled up to the frequencies about 1.3 THz for d = 200 μm or up to 0.3 THz for d = 800 μm. The best phase-matching is for the *oo–e* interaction. However, as is shown below, the effective nonlinearity and reflection angular dependencies make the *ee–e* interaction the most efficient one. The type II *oe–e* and *oe–o* interactions are the only ones for which

there is a narrow frequency range with ideal phase matching (Δk = 0) (Figure 4b). The phase-matching angles θ of more than 20 degrees are not reasonable as the phase matching shifts to overly high frequencies. Increasing the θ angle increases the terahertz frequencies for which the phase matching is fulfilled. As it can be seen, the thicker crystal is taken, and the lower phase mismatch is required to yield the condition (4). Thus, for the thick crystals, the spectral range of phase matching at a given angle becomes narrower. This can be used to obtain narrowband terahertz generation. Finally, the *eo–e* and *eo–o* interactions are less interesting ones for practical realization. Only small θ angles that are below 10° provide phase matching (Figure 4c). As the internal θ angles are used in Figure 4a–c, we also show the internal θ angle dependence on the external angle of incidence for the (001) $ZnGeP_2$ crystals in Figure 4d.

Besides the phase-matching the terahertz generation by the optical rectification in a nonlinear crystal depends on the crystal's thickness, absorption coefficient at the pump and generated terahertz wavelengths, Fresnel's reflection and effective nonlinearity. In the case of terahertz generation by optical rectification of a femtosecond laser pulse, the widely used slowly varying amplitude approximation is not applicable. In order to model the terahertz generation spectra, we used the approach proposed in [25,26] where the amplitude of the generated terahertz wave is written as:

$$E_{THz}(\nu) \sim d_{eff} A_{1g}^2 F_0(\nu, \tau) G(\nu, \lambda, d) \quad (8)$$

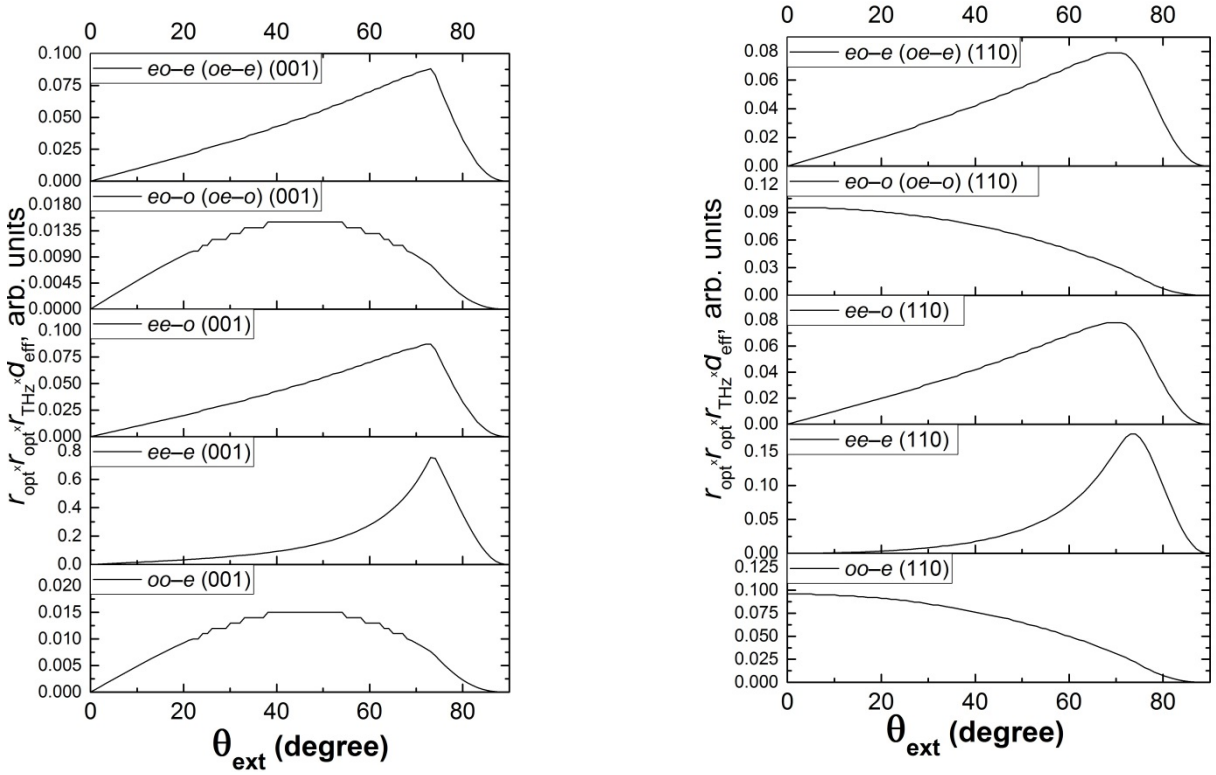
Here, d_{eff} is the effective nonlinearity of the second order (for $ZnGeP_2$ is given in Table 1 for all of the possible interactions), $A_{1\text{g}}$ is the pump pulse electric field amplitude, and $F_0(\omega, \tau) \sim \omega^2 \exp(-(\omega\tau)^2/2)$ describes the effect of the spectral width and duration of the laser pulse. In the calculations, τ = 120 fs was used. The influence of the phase-matching conditions $\Delta k(\lambda, \nu, \theta)$, the absorption coefficients in the visible and terahertz ranges $\alpha_{opt}, \alpha_{THz}$ and the crystal thickness d on the emitted spectral waveform are gathered in the function:

$$G(\nu, \lambda, d, \theta) = \frac{e^{id[\Delta k(\nu,\lambda,\theta) + i\alpha_{THz}(\nu)]} - 1}{i[\Delta k(\nu, \lambda, \theta) + i\alpha_{THz}(\nu)]} e^{-i\alpha_{opt} d} \quad (9)$$

Table 1. Effective nonlinearities in $ZnGeP_2$ for all of the possible three-wave interactions.

Interaction	d_{eff}
oo–o	0
oo–e	$-d_{36} \sin(\theta) \sin(2\phi)$
ee–o	$d_{14} \sin(2\theta) \cos(2\phi)$
ee–e	$-(2d_{14} + d_{36}) \cos^2(\theta) \sin(\theta) \sin(2\phi)$
oe–e (*eo–e*)	$\frac{1}{2}(d_{14} + d_{36}) \sin(2\theta) \cos(2\phi)$
eo–o (*oe–o*)	$-d_{14} \sin(\theta) \sin(2\phi)$

The pump pulse electric field amplitudes $A_{1\text{g}}$ and E_{THz} (ν) will definitely depend also on the Fresnel's reflection losses. We have plotted the dependencies on the external incidence angle of the product of all of the reflection losses and effective nonlinearity for the (001) and (110) $ZnGeP_2$ crystals without antireflection coatings in Figure 5a,b. In both of the cases, the *ee–e* interaction at the θ angle close to the Brewster angle (about 74°) seems to be optimal. For the (110) $ZnGeP_2$ slabs also, the *oo–e* interaction at a normal incidence is advantageous.



(**a**) (**b**)

Figure 5. (**a**) The dependence of the product of all reflection losses and effective nonlinearity on external angle of incidence for all possible interactions for (100) (**a**) and (110) (**b**) $ZnGeP_2$ crystals.

The measured and calculated terahertz spectra which were generated in the annealed $ZnGeP_2$ crystals of thicknesses 200, 500 and 800 μm by *ee–e* and *oe–e* optical rectification are presented in Figure 6. For each interaction, all of the spectra are normalized to the maximal spectral amplitude of the most efficient conversion (θ = 55° *d* = 200 μm for *ee–e* and θ = 55° *d* = 800 μm for *oe–e* type model and θ = 45° *d* = 800 μm for *oe–e* type experiment). It is seen that the model reproduces the main features of the experimental spectra; the discrepancies are, first of all, due to the spectral dependence of the detection efficiency (which was not included in the model). The detection efficiency is lower for the frequencies that are above 2 THz. Additionally, the walk-off (arising for *e*-waves) was not accounted for. The walk-off probably explains the fact that while θ = 74° at *ee–e* is the optimal angle according to the calculations, experimentally, the highest signal was measured at θ = 55–60°.

In the next step, we experimentally checked the possibility to achieve the narrowing of the terahertz generation bandwidth at the *oe–e* interaction in the thicker $ZnGeP_2$ (*d* = 2015 μm) crystal. The modeled and measured terahertz generation spectra are shown in Figure 7a in comparison with those which were obtained in the *d* = 200 μm crystal. Finally, the terahertz generation in the $ZnGeP_2$:Sc crystals was tested. The prepared slabs had a (110) orientation. For these samples, the *oo–e* interaction at a normal incidence was deduced to be efficient. The obtained experimental and modeled spectra are given in Figure 7b. Taking into account the lower $\alpha_{opt}, \alpha_{THz}$ of the Sc-doped crystal, the higher efficiency was expected. The experimentally measured efficiency is even higher when it is compared to that for reference crystal (pure $ZnGeP_2$ N2) than it was predicted to be by the models.

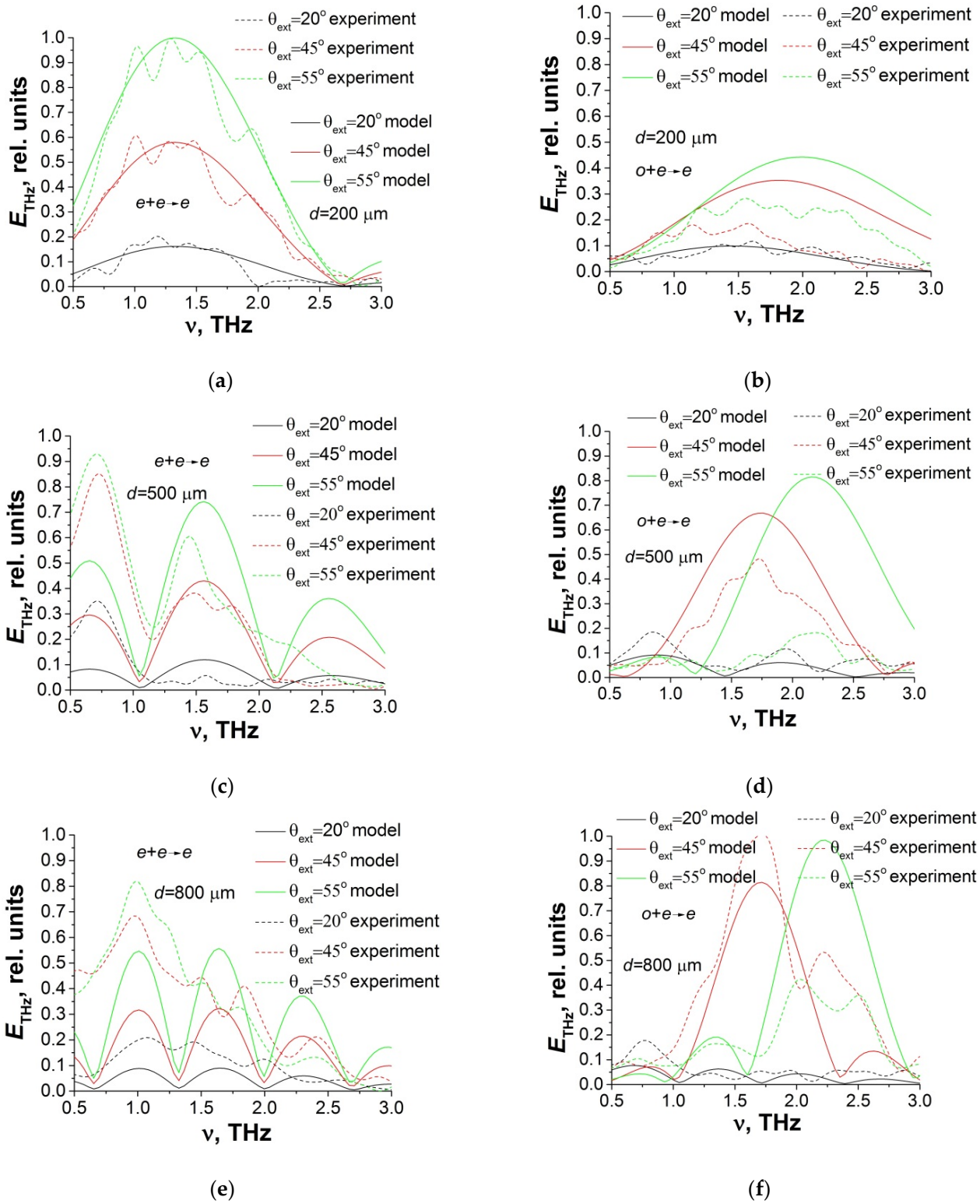
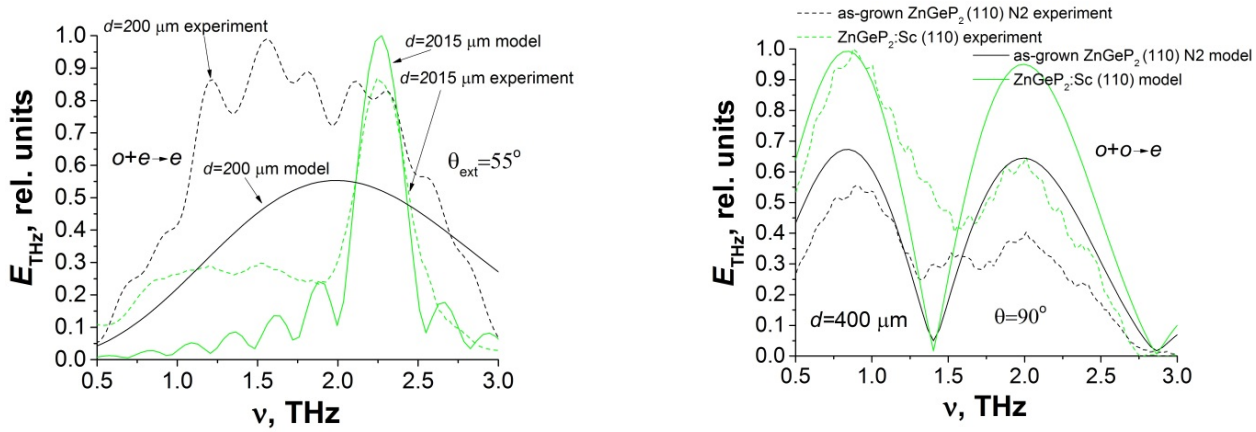


Figure 6. Measured (dashed lines) and modeled (solid lines) terahertz generation spectra obtained by optical rectification at *ee*–*e* and *oe*–*e* interactions in annealed $ZnGeP_2$ of thickness 200 μm (**a**,**b**), 500 μm (**c**,**d**) and 800 μm (**e**,**f**). Experimental configurations are given in the legends.



(**a**) (**b**)

Figure 7. Measured (dashed lines) and modeled (solid lines) terahertz generation spectra obtained by optical rectification at *oe*–*e* interaction in annealed $ZnGeP_2$ of thicknesses 200 μm and 2015 μm (**a**) and at *oo*–*e* interaction in (110) $ZnGeP_2$ and $ZnGeP_2$:Sc of thickness 400 μm (**b**). Experimental configurations are given in the legends.

4. Conclusions

Terahertz wave generation through the optical rectification of 780 nm femtosecond laser pulses in $ZnGeP_2$ crystals has been studied. All of the possible interactions of types I and II were studied by modeling and in experiments. The possibility of broadband "low-frequency" terahertz generation by *ee*–*e* interaction and "high-frequency" terahertz generation by *oe*–*e* interaction was demonstrated. The possibility to achieve the narrowing of the terahertz generation bandwidth at the *oe*–*e* interaction using thicker $ZnGeP_2$ crystals was experimentally confirmed for a 2-mm-thick crystal. It was found that the thermal annealing of the as-grown $ZnGeP_2$ crystals and their doping with a 0.01 mass % of Sc reduces the absorption in the "anomalous absorption" region (λ = 0.62–3 μm). The terahertz generation by the *oo*–*e* optical rectification in (110) $ZnGeP_2$:Sc and the as-grown $ZnGeP_2$ crystals of equal thickness has been compared. It has been found that $ZnGeP_2$:Sc is more efficient for 780 nm femtosecond laser pulses optical rectification.

Author Contributions: Conceptualization, V.V., Y.S.S. and S.Y.S.; methodology, S.B. and S.Y.S.; software, S.Y.S.; validation, Y.S.S. and S.Y.S.; formal analysis, S.Y.S.; investigation, V.V., S.B., N.N.Y., V.V. and S.Y.S.; resources, V.V., S.B. and N.N.Y.; data curation, S.Y.S.; writing—original draft preparation, S.Y.S.; writing—review and editing, S.Y.S.; visualization, S.Y.S.; supervision, S.Y.S.; project administration, S.Y.S.; funding acquisition, S.Y.S. All authors have read and agreed to the published version of the manuscript.

Funding: This work was supported by the Ministry of Science and Higher Education of the Russian Federation (project No FSWM-2020-0038). This study was also supported by a grant under the Decree of the Government of the Russian Federation No. 220 of 9 April 2010 (Agreement No. 075-15-2022-1132 on 1 July 2022).

Institutional Review Board Statement: Not applicable.

Informed Consent Statement: Not applicable.

Data Availability Statement: Not applicable.

Acknowledgments: The part of the research related to the phase-matching analysis and study of terahertz generation in the nonlinear crystals was supported by the Ministry of Science and Higher Education of the Russian Federation (project No FSWM-2020-0038). The part of the research related to the crystal growth and measurement of their optical properties was carried out with the support of a grant under the Decree of the Government of the Russian Federation No. 220 of 9 April 2010 (Agreement No. 075-15-2022-1132 on 1 July 2022).

Conflicts of Interest: The authors declare no conflict of interest.

References

1. Goryunova, N.A. *Complex Diamond-Like Semiconductors*; Sov. Radio: Moscow, Russia, 1968. (In Russian)
2. Boyd, G.D.; Buehler, E.; Storz, F.G. Linear and nonlinear optical properties of $ZnGeP_2$ and CdSe. *Appl. Phys. Lett.* **1971**, *18*, 301–304. [CrossRef]
3. Vodop'yanov, K.L.; Voevodin, V.G.; Gribenyukov, A.I.; Kulevskii, L.A. High-efficiency picosecond parametric superradiance emitted by a $ZnGeP_2$ crystal in the 5–6.3 μm range. *Quantum Electron.* **1987**, *17*, 1159–1161.
4. Lei, Z.; Zhu, C.; Xu, C.; Yao, B.; Yang, C. Growth of crack-free $ZnGeP_2$ large single crystals for high-power mid-infrared OPO applications. *J. Cryst. Growth* **2014**, *389*, 23–29. [CrossRef]
5. Zawilski, K.T.; Schuneman, P.G.; Setzler, S.D.; Pollak, T.M. Large aperture single crystal $ZnGeP_2$ for high-energy applications. *J. Cryst. Growth* **2008**, *310*, 1891–1896. [CrossRef]
6. Verozubova, G.A.; Gribenyukov, A.I.; Korotkova, V.V.; Ruzaikin, M.P. $ZnGeP_2$ synthesis and growth from melt. *Mater. Sci. Eng. B* **1997**, *48*, 191–197. [CrossRef]
7. Brudnyi, V.N.; Budnitskii, D.L.; Krivov, M.A.; Masagutova, R.V.; Prochukhan, V.D.; Rud, Y.V. The electrical and optical properties of 2.0 MeV electron-irradiated $ZnGeP_2$. *Phys. Status Solidi* **1978**, *50*, 379–384. [CrossRef]
8. Gribenyukov, A.I.; Voevodin, V.I. Influence of the preparation conditions on optical properties of single crystals $ZnGeP_2$ in THz range. *J. Phys. Conf. Ser.* **2018**, *1115*, 052030. [CrossRef]
9. Yang, Y.; Zhang, Y.; Gu, Q.; Zhang, H.; Tao, X. Growth and annealing characterization of $ZnGeP_2$ crystal. *J. Cryst. Growth* **2011**, *318*, 721–724. [CrossRef]
10. Yue, X.; Xu, M.; Du, W.; Chu, C. Surface finishing of $ZnGeP_2$ single crystal by diamond tool turning method. *Opt. Mater.* **2017**, *71*, 141–144. [CrossRef]
11. Ding, Y.J.; Shi, W. Widely tunable monochromatic THz sources based on phase-matched difference-frequency generation in nonlinear-optical crystals: A novel approach. *Laser Phys.* **2006**, *16*, 562–570. [CrossRef]
12. Bereznaya, S.A.; Korotchenko, Z.V.; Redkin, R.A.; Sarkisov, S.Y.; Tolbanov, O.P.; Trukhin, V.N.; Gorlenko, N.P.; Sarkisov, Y.S.; Atuchin, V.V. Broadband and narrowband terahertz generation and detection in $GaSe_{1-x}S_x$ crystals. *J. Opt.* **2017**, *19*, 115503. [CrossRef]
13. Nazarov, M.M.; Sarkisov, S.Y.; Shkurinov, A.P.; Tolbanov, O.P. $GaSe_{1-x}S_x$ and $GaSe_{1-x}Te_x$ thick crystals for broadband terahertz pulses generation. *Appl. Phys. Lett.* **2011**, *99*, 081105. [CrossRef]
14. Zelmon, D.E.; Hanning, E.A.; Schunemann, P.G. Refractive-index measurements and Sellmeier coefficients for zinc germanium phosphide from 2 to 9 μm with implications for phase matching in optical frequency-conversion devices. *J. Opt. Soc. Am.* **2001**, *18*, 1307–1310. [CrossRef]
15. Chuchupal, S.V.; Komandin, G.A.; Zhukova, E.S.; Prokhorov, A.S.; Porodinkov, O.E.; Spektor, I.E.; Shakir, Y.A.; Gribenyukov, A.I. Mechanisms of loss formation in nonlinear optical crystals $ZnGeP_2$ in the terahertz frequency range. *Phys. Sol. State* **2014**, *56*, 1391–1396. [CrossRef]
16. Voevodin, V.I.; Yudin, N.N.; Sarkisov, S.Y. Influence of thermal annealing on terahertz dielectric properties of $ZnGeP_2$ crystals. *Russ. Phys. J.* **2021**, *64*, 1513–1516. [CrossRef]
17. Li, F.; Zhong, K.; Qiao, H.; Liu, K.; Zhang, X.; Xu, D.; Yao, J. Efficient tunable terahertz generation via noncollinear phase matching in the $ZnGeP_2$ crystal. *J. Opt. Soc. Am. B* **2020**, *37*, 3857–3864. [CrossRef]
18. Piyathilaka, H.P.; Sooriyagoda, R.; Dewasurendra, V.; Johnson, M.B.; Zawilski, K.T.; Schunemann, P.G.; Bristow, A.D. Terahertz generation by optical rectification in chalcopyrite crystals $ZnGeP_2$, $CdGeP_2$ and $CdSiP_2$. *Opt. Exp.* **2019**, *27*, 16958–16965. [CrossRef]
19. Carnio, B.N.; Hopmann, E.; Zawilski, K.T.; Schunemann, P.G.; Elezzabi, A.Y. Chalcopyrite and chalcogenide crystals for terahertz radiation generation and detection. *Proc. SPIE* **2021**, *11670*, 84–89.
20. Kolesnikova, I.A.; Kobtsev, D.A.; Redkin, R.A.; Voevodin, V.I.; Tyazhev, A.V.; Tolbanov, O.P.; Sarkisov, Y.S.; Sarkisov, S.Y.; Atuchin, V.V. Optical pump—THz probe study of HR GaAs:Cr and SI GaAs:EL2 structures with long charge carrier lifetimes. *Photonics* **2021**, *8*, 575. [CrossRef]
21. Redkin, R.A.; Kobtsev, D.A.; Bereznaya, S.A.; Korotchenko, Z.V.; Sarkisov, Y.S.; Mihaylov, T.A.; Sarkisov, S.Y. GaSe crystals with antireflection coatings for terahertz generation. *Mater. Res. Express* **2019**, *6*, 126201. [CrossRef]
22. Hagner, M.; Sulzer, P.; Liehl, A.; Cimander, M.; Kempf, H.; Bitzer, A.; Herter, A.; Leitenstorfer, A. Ultrabroadband suppression of mid-infrared reflection losses of a layered semiconductor by nanopatterning with a focused ion beam. *Opt. Exp.* **2021**, *29*, 33632–33641. [CrossRef] [PubMed]

23. Bhar, G.C.; Samanta, L.K.; Ghosh, D.K.; Das, S. Tunable parametric $ZnGeP_2$ crystal oscillator. *Sov. J. Quantum Electron.* **1987**, *17*, 860–861. [CrossRef]
24. Dexheimer, S.L. (Ed.) *Terahertz Spectroscopy: Principles and Applications*; CRC Press: Boca Raton, FL, USA, 2008. [CrossRef]
25. Nazarov, M.M.; Makarova, S.A.; Shkurinov, A.P.; Okhotnikov, O.G. The use of combination of nonlinear optical materials to control terahertz pulse generation and detection. *Appl. Phys. Lett.* **2008**, *92*, 021114. [CrossRef]
26. Kitaeva, G.K. Terahertz generation by means of optical lasers. *Laser Phys. Lett.* **2008**, *5*, 559–576. [CrossRef]